ELSEVIER

Agricultural and Forest Meteorology 91 (1998) 39–49

AGRICULTURAL AND FOREST METEOROLOGY

On micrometeorological observations of surface-air exchange over tall vegetation

Xuhui Lee*

School of Forestry and Environmental Studies, Yale University, New Haven, Connecticut 06511, USA

Received 14 October 1997; received in revised form 18 February 1998; accepted 20 February 1998

Abstract

It is shown from the mass conservation and the continuity equations that the net ecosystem exchange (NEE) of a scalar constituent with the atmosphere should be

$$\mathrm{NEE} = \int_0^{z_r} \frac{\partial \bar{c}}{\partial t} \mathrm{d}z + \left(\overline{w'c'}\right)_r + \bar{w}_r \left(\bar{c}_r - \frac{1}{z_r} \int_0^{z_r} \bar{c} \mathrm{d}z \right)$$

where the first term on RHS is the storage below the height of observation (z_r), the second term is the eddy flux, and the third term is a mass flow component arising from horizontal flow convergence/divergence or a non-zero mean vertical velocity ($\bar{w}_r$) at height z_r. The last term, unaccounted for in previous studies of surface-air exchanges, becomes important over tall vegetation and at times when the vertical gradient of the atmospheric constituent $(\bar{c}_r - (1/z_r)\int_0^{z_r} \bar{c}\mathrm{d}z)$ is large, as is the case with CO_2 in forests at night. Experimental evidence is presented to support the postulation that the mass flow component is in large part responsible for the large run-to-run variations in eddy fluxes, the lack of energy balance closure and the apparent low eddy fluxes at night under stable stratifications. Three mechanisms causing the non-zero mean vertical velocity are discussed. Of these, drainage flow on undulating terrain is the most important one for long-term flux observations because only a small terrain slope is needed to trigger its occurrence. It is suggested from the data obtained at a boreal deciduous forest that without proper account of the mass flow component, the assessment of annual uptake of CO_2 could be biased significantly towards higher values. It is argued that quantifying the mass flow component is a major challenge facing the micrometeorological community. © 1998 Elsevier Science B.V. All rights reserved.

Keywords: Net ecosystem exchange; Drainage; CO_2; Forest

1. Introduction

In recent years micrometeorological techniques have been widely used in observational studies of CO_2 uptake by terrestrial ecosystems (Goulden et al., 1996a; Black et al., 1996; Grace et al., 1995), air-vegetation exchanges of pollutants (Fuentes et al., 1992; Guenther et al., 1996) and trace metals (Lindberg et al., 1997), and ecosystem processes (Baldocchi and Harley, 1995; Hollinger et al., 1994; Verma et al., 1986). One major concern with the

*Corresponding author. Tel.: (203)432-6271; fax: (203)432-3929; e-mail: xuhui.lee@yale.edu

0168-1923/98/$19.00
PII S0168-1923(98)00071-9

observations is the lack of energy balance closure and the large run-to-run variations in scalar fluxes, a problem that is particularly serious over tall vegetation. Mechanisms such as advection due to inadequate fetch (Moore and Hicks, 1973; Fitzjarrald and Moore, 1994), a mismatch of net radiometer and eddy correlation (EC) footprints (Moore et al., 1996), instrument uncertainties (Shuttleworth et al., 1988; Thompson, 1979), and descending motion associated with stationary convective cells (Lee and Black, 1993b) have been proposed as possible causes of the problem. A thorough survey of the problem can be found in Mahrt (1998).

Another problem in the forest environment, frequently encountered at nights of low wind speed, is the apparent low EC flux. The best example for this is provided by CO_2 flux observations (Goulden et al., 1996b; Jarvis et al., 1997). Possible causes of the problem include drainage flow (Grace et al., 1996), advection (Sun et al., 1997), line averaging and tube attenuation (Moncrieff et al., 1996; Leuning and Judd, 1996)

The objective of this study is to examine the effect of a non-zero mean vertical velocity or horizontal flow divergence/convergence on the atmospheric exchange over forests. Central to the study is a formulation for the net ecosystem exchange (NEE) of a scalar constituent with the atmosphere derived from the mass conservation equation. It is shown in Section 2 that a non-zero mean vertical velocity at the height of flux observations will lead to a significant additional mass flow component of NEE unaccounted for by previous studies. Data from two forest turbulence experiments, one at Browns River (BR, Lee and Black, 1993a, b) and the other at Prince Albert (PA, Black et al., 1996; Lee et al., 1997; Blanken et al., 1997), are analyzed in Section 3 to support this new formulation. BR is a case dominated by highly convective motions, while PA data suggests the existence of a negative vertical velocity at night, indicative of drainage flow, even though the site was thought to be sufficiently flat and uniform to meet micrometeorological flux observation criteria. Finally, Section 4 presents a discussion of several important mechanisms responsible for the non-zero mean vertical velocity and explores their implications for quantifying NEE of CO_2 between the atmosphere and the forest vegetation.

2. Theory

Almost all micrometeorological studies of surface–air exchange assume a zero mean vertical velocity or zero dry air flux. While this may be a good assumption very close to the ground, there are many reasons to question its validity over tall vegetation. For example, the horizontal divergence rate frequently used for scale analysis of synoptic weather systems is $10^{-5}\ \mathrm{s}^{-1}$ (Wallace and Hobbs, 1977), which amounts to a vertical velocity of $-0.04\ \mathrm{cm\ s}^{-1}$ at the height of 40 m above the ground, or roughly two tree heights. (In the following, this height is taken as a typical height for observations of surface-air exchange over forests.) The vertical velocity associated with local thermal circulations (Segal et al., 1988; Mahrt and Ek, 1993; Sun et al., 1997), topographically modified flow (Finnigan and Brunet, 1995), and divergence in convective cell-like structures will be at least an order of magnitude larger. An extended discussion on this subject is given in Section 4.

To quantify the effect of the non-zero vertical velocity on NEE, we begin with the conservation equation of a scalar c in the x–z plane, ignoring the molecular term

$$\frac{\partial c}{\partial t}+\frac{\partial (uc)}{\partial x}+\frac{\partial (wc)}{\partial z}=s \quad (1)$$

where axis x is aligned with the mean wind direction and axis z is perpendicular to the local terrain surface, s is a source term, and u and w are the velocity components in the x and z directions, respectively. After Reynolds decomposition and averaging, Eq. (1) leads to

$$\frac{\partial \bar{c}}{\partial t}+\frac{\partial \overline{u'c'}}{\partial x}+\bar{u}\frac{\partial \bar{c}}{\partial x}+\bar{c}\frac{\partial \bar{u}}{\partial x}+\frac{\partial \overline{w'c'}}{\partial z}+\frac{\partial (\bar{w}\bar{c})}{\partial z}=s \quad (2)$$

where primes denote departures from the mean, and overbars denote time averaging. A more rigorous treatment of the averaging procedure can be found in Finnigan (1985). The air is assumed to be incompressible so that

$$\frac{\partial \bar{u}}{\partial x}=-\frac{\partial \bar{w}}{\partial z}\simeq -\frac{\bar{w}_r}{z_r} \quad (3)$$

where $\bar{w}_r$ is the mean vertical velocity at the height of flux observation (z_r). Assuming no divergence of horizontal eddy flux (term 2 on LHS of Eq. (2) = (0)

and no horizontal advection (term 3=0) and using Eq. (3), the integration of Eq. (2) with respect to z yields

$$\begin{aligned}\mathrm{NEE} &\equiv \int_0^{z_r} s\mathrm{d}z + (\overline{w'c'})|_{z=0} \\ &= \int_0^{z_r} \frac{\partial \bar{c}}{\partial t}\mathrm{d}z + (\overline{w'c'})_r + \bar{w}_r(\bar{c}_r - \langle \bar{c} \rangle)\end{aligned} \tag{4}$$

where subscript r denotes a quantity at height z_r and $\langle \bar{c} \rangle$ is the averaged concentration between the ground and this height.

Eq. (4) illustrates that NEE should consist of three components, storage below the height of observation (term 1 on RHS), eddy flux (term 2) and a mass flow component arising from the horizontal flow divergence/convergence or a non-zero mean vertical velocity (term 3). The last term, somewhat analogous to a bulk heat deficit term due to nocturnal subsidence (Carlson and Stull, 1986), can be understood by considering a volume of air over the EC footprint as shown in Fig. 1. Suppose that the scalar concentration decreases with increasing height, typical for CO_2 in forests at night, and that $\bar{w}_r$ is negative. To satisfy the continuity requirement, the negative $\bar{w}_r$ must be balanced by a horizontal flow divergence. Air entering the volume from above carries less CO_2 than air moving out from the sides by divergence, causing a net depletion of CO_2 below z_r. Conversely, a positive $\bar{w}_r$ will cause a net accumulation in the air volume. Obviously the mass flow component becomes significant when the vertical change in the concentration is large. Since the mean vertical velocity is proportional to height (Eq. (3)), the mass flow effect on the flux observation over tall vegetation will be much more pronounced than over short vegetation.

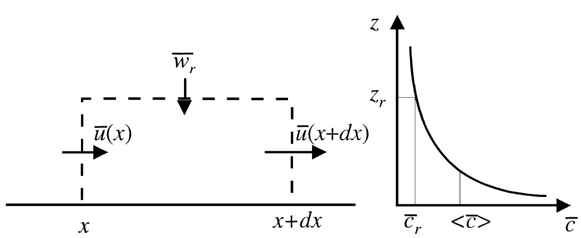

Fig. 1. Schematic diagram illustrating the effect of a non-zero vertical velocity on the surface-air exchange. Air entering the air volume from above is balanced by a horizontal flow divergence. This will result in a net depletion of the scalar mass from the air volume if the mean scalar concentration decreases with increasing height.

Moncrieff et al. (1996) and Sun et al. (1997) treat the problem in a slightly different manner. They consider the term $\partial(\bar{u}\bar{c})/\partial x$ instead of $\bar{u}(\partial\bar{c}/\partial x)$ as in this study to be the advection term. It is believed that the advection effect is confined to small areas downwind of the transitional boundary of the surface source and can be minimized by choosing the site following the usual fetch and footprint criteria. However, the mass flow component can be significant even at an extensive and uniform site. An example is given in Section 4 that compares the relative importance of the advection and mass flow terms for the HAPEX-MOBILHY forest.

3. Energy imbalance

3.1. Correcting mean vertical velocity of sonic anemometers

It is not appropriate to directly use the mean vertical velocity measured by 3D sonic anemometers in evaluating the mass flow component because the signal level is very low and can be contaminated by even a slight zero offset in the electronics, the sensor tilt relative to the terrain surface and the aerodynamic shadow of the sensor structure. The problem can be represented by a linear equation to a good approximation as

$$\hat{w} = \bar{w} + a(\phi) + b(\phi)\hat{u} \tag{5}$$

where $\hat{w}$ and $\hat{u}$ are the measured mean vertical and horizontal velocities in the instrument coordinate, respectively, $\bar{w}$ is the true mean vertical velocity (the velocity component along the direction normal to the local terrain surface), and a and b are wind direction (ϕ) dependent coefficients. A further crude approximation is that $\bar{w}$ behaves in a random fashion so that the data ensemble can be used to evaluate a and b by a least squares method. Once the coefficients are known, Eq. (5) is used to find $\bar{w}$ for each run. This correction procedure will however cause a systematic bias if air at the site has a preferred direction of vertical motion, a point that should be kept in mind when interpreting the results below.

The wind direction at BR was very steady during the whole experiment. The same a and b values, found by regression of $\hat{w}$ against $\hat{u}$ using the whole data set, are used to correct the vertical velocity measurement for all the runs. For the PA site, data obtained during 2 August–19 September 1994, a period when both EC and profile sensors were functioning properly, is chosen for this study. Values of a and b at PA are found as functions of ϕ at 1° increments by linear regression using a subset of the runs (>100 runs) whose wind directions fall within $\phi \pm 7°$. Correction to the vertical velocity is made with the appropriate a and b values. The corrected mean vertical velocity does not show either dependence on ambient conditions (temperature and wind speed) or a long-term trend over the period of observations.

Fig. 2 compares the corrected vertical velocities at two EC heights. Observation at BR was conducted in the daytime only while data at PA include both daytime and nighttime runs. Of importance is the feature that the data follow a line with a slope equal to the ratio of the two measurement heights as suggested by Eq. (3). The result indicates that the correction procedure works reasonably well on the whole, but a large scatter is also evident.

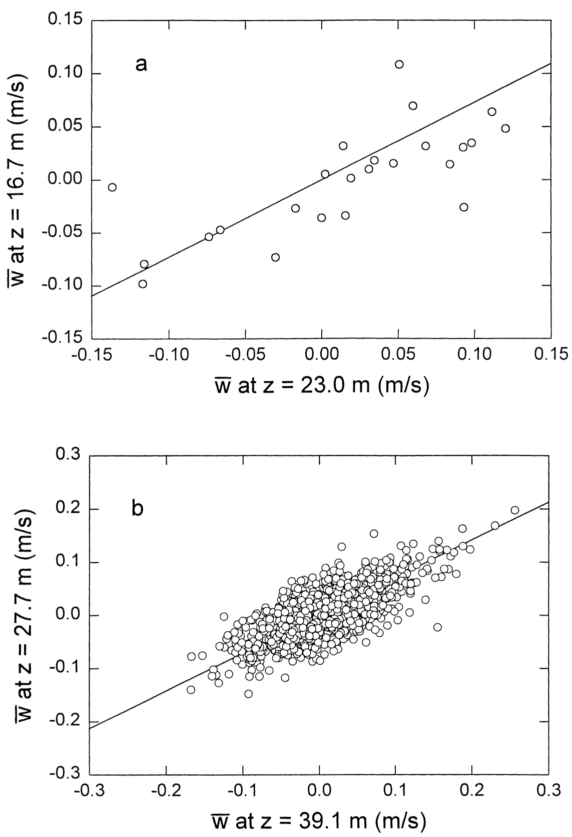

Fig. 2. Comparison of the corrected 30 min mean vertical velocity at two heights at BR (a) and PA (b). The lines represent a slope equal to the ratio of the two measurement heights.

3.2. Energy imbalance

Applying Eq. (4) to sensible heat and water vapor exchanges, one obtains

$$H = \int_0^{z_r} \frac{\partial \bar{T}}{\partial t} \mathrm{d}z + \overline{w'T'} + \bar{w}_r(\bar{T}_r - \langle \bar{T} \rangle) \qquad (6)$$

$$E = \int_0^{z_r} \frac{\partial \bar{\rho}_\mathrm{v}}{\partial t} \mathrm{d}z + \overline{w'\rho_\mathrm{v}'} + \bar{w}_r(\bar{\rho}_{\mathrm{v}r} - \langle \bar{\rho}_\mathrm{v} \rangle) \qquad (7)$$

where H and E are the net ecosystem exchanges of kinematic sensible heat and water vapor, respectively, T is air temperature and ρ_v is water vapor density. The complete energy balance equation becomes

$$R_\mathrm{n} - S - G = \rho c_\mathrm{p} \overline{w'T'} + \lambda \overline{w'\rho_\mathrm{v}'} + \bar{w}_r \delta \qquad (8)$$

where R_n is net radiation flux density over the forest, ρ is air density, c_p is the specific heat of air at constant pressure, λ is latent heat of vaporization, G is heat flux into the soil, $\delta = \rho c_\mathrm{p}(\bar{T}_r - \langle \bar{T} \rangle) + \lambda(\bar{\rho}_{\mathrm{v}r} - \langle \bar{\rho}_\mathrm{v} \rangle)$, and S is a heat storage term including sensible and latent heat storage in the air and heat storage in the biomass. Thermodynamic quantity δ is generally negative in the daytime and positive at night, with typical values of -2000 and $500\ \mathrm{J\ m^{-3}}$ around noon and midnight hours, respectively (Fig. 3). As an example, a mean vertical velocity of $5\ \mathrm{cm\ s^{-1}}$ at the EC height will produce equivalent energy fluxes of -100 and $25\ \mathrm{W\ m^{-2}}$ for daytime and nighttime, respectively, or an uncertainty of roughly 20% of the observed net radiation flux in the conventional energy balance analysis which ignores the mass flow effect.

In contrast to the tall vegetation, the mass flow problem is less serious over short canopies. Using the idealized profiles representative of a cereal crop growing to a height of 1 m (Monteith and Unsworth, 1990) and assuming the EC measurements are made at z=2 m, the daytime values (nighttime values in brackets) for δ and $\Delta\bar{C}(= \bar{C}_r - \langle \bar{C} \rangle$, CO_2 concentration gradient) are estimated to be $-2400\ \mathrm{J\ m^{-3}}$ ($2000\ \mathrm{J\ m^{-3}}$) and $1\ \mathrm{mg\ m^{-3}}$ ($-10\ \mathrm{mg\ m^{-3}}$). If

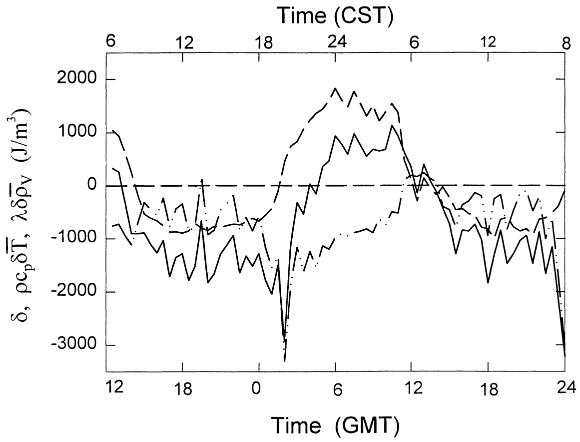

Fig. 3. An example showing the diurnal variations in the thermodynamic properties δ (solid line), $\rho c_p \delta \bar{T} = \rho c_p(\bar{T}_r - \langle \bar{T} \rangle)$ (dash line), and $\lambda \delta \bar{\rho}_v = \lambda(\bar{\rho}_{vr} - \langle \bar{\rho}_v \rangle)$ (dash–dot line) at PA on August 8–9, 1994, where subscript r denote values at the EC height (39.1 m above the ground).

$5\ \mathrm{cm\ s^{-1}}$ is typical for $\bar{w}$ at the 40 m height, the corresponding value at z=2 m will be $0.25\ \mathrm{cm\ s^{-1}}$ according to Eq. (3). Both energy and CO_2 fluxes resulting from the mass flow are quite small (daytime and nighttime energy fluxes of −6 and $5\ \mathrm{W\ m^{-2}}$, respectively, and CO_2 fluxes of 0.0025 and −0.025 mg (CO_2) $\mathrm{m^{-2}\ s^{-1}}$, respectively).

Eq. (8) shows that a negative $\bar{w}$ will lead to a positive energy imbalance defined as $I = R_n - S - G - \rho c_p \overline{w'T'} - \lambda \overline{w'\rho_v'}$ in the daytime or in other words, a negative correlation should exist between $\bar{w}$ and I. This deduction is confirmed by both BR and PA data shown in Fig. 4(a) and (b). In Fig. 4, the mean vertical velocity has been corrected using the procedure above. (Data from morning and evening transitional periods are excluded from the analysis.) The correlation is significant at a confidence level <0.001. The correlation for nighttime runs is positive (Fig. 4(c)), again in accord with Eq. (8), with a larger relative scatter (confidence level 0.01) expected for measurements of energy balance components of small magnitude at night.

However, the attempt to evaluate the mass flow component for individual runs using the corrected mean w and measured temperature and humidity profiles has brought an improvement only by a moderate amount of 20% to the nighttime energy balance at PA and no improvement to the daytime energy balance at either site. The difficulty is mainly a consequence of the fact that the mass flow component is a product of two independent quantities, both suffering from large measurement uncertainties. Addi-

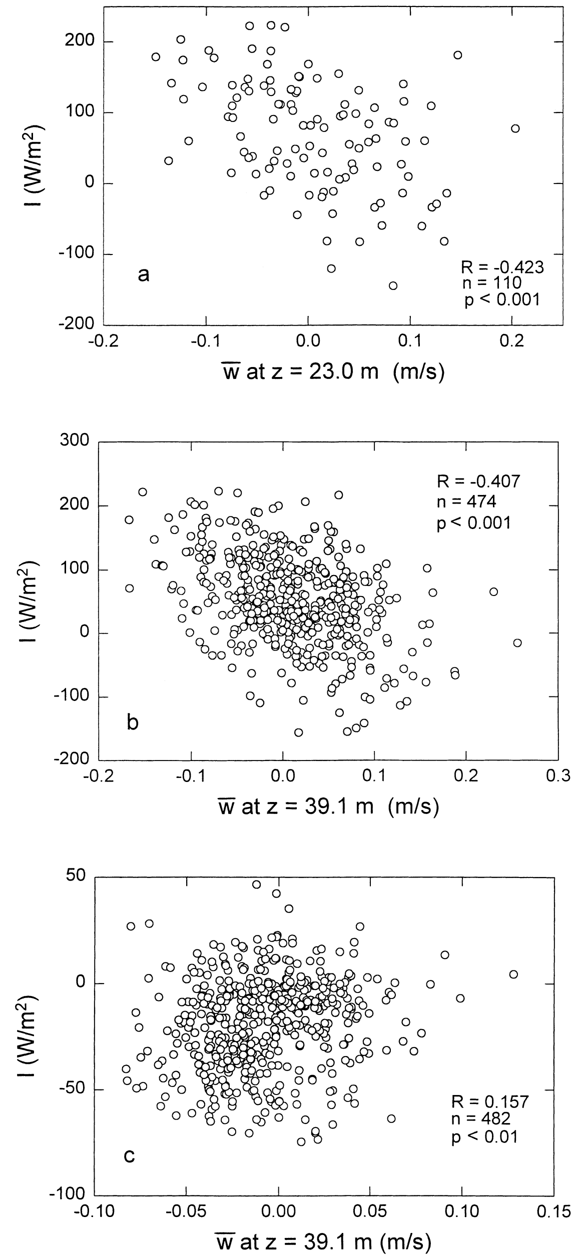

Fig. 4. Scatter plot showing the influence of the mean vertical velocity ($\bar{w}$) on the energy imbalance (I): (a) period 09–17 PST at BR; (b) period 10–16 CST at PA; (c) period 22–04 CST at PA.

tionally, the w correction method does not allow a non-zero value for the long-term averaged mean vertical velocity, which as noted above, will introduce a systematic bias to the evaluation if the site generates a preferred direction of vertical motion.

4. Qualitative discussion

4.1. Mechanisms responsible for non-zero $\bar{w}$

4.1.1. Convection

It is a well-known phenomenon in the convective boundary layer that ascending motion is confined to thin walls surrounding large columns of relatively slow descending motion at a horizontal scale of 1–2 km (Stull, 1988; Garratt, 1992). Vertical velocities as large as 10 cm s^{-1} are possible at 40 m above the ground within the descending air column according to the simulation study of Moeng (1984). The large eddy simulation of Schmidt and Schumann (1989) suggests that the area ratio is roughly 10%, while the estimate given by Emanuel (1994) for precipitating deep convection is 0.3%. The probability for micrometeorological tower instruments to be influenced by descending motion is therefore much higher than by ascending motion. For example, Garstang et al. (1990) found that, even in the wet season, divergence (descending motion) can dominate over convergence (ascending motion) in both magnitude and duration over a forested area in the Amazon. The probability is even higher if we consider the fact that micrometeorological flux towers are almost always situated in uniform forests while ascending motion is most likely to occur over localized hot spots such as roads and small clearings as postulated by Stull (1988) and suggested by the large eddy simulation of Shen and Leclerc (1995).

In a spatial domain, the total surface-air flux is composed of turbulence and mesoscale components (Mahrt and Sun, 1995; Avissar and Chen, 1993). Micrometeorological fluxes observed at a single point can be spatially representative if these column-like structures propagate past the sensors at a reasonable speed so that the vertical velocity averaged over the Reynolds averaging interval vanishes. Under highly convective conditions (low friction velocity and low wind speed), however, these structures are more likely

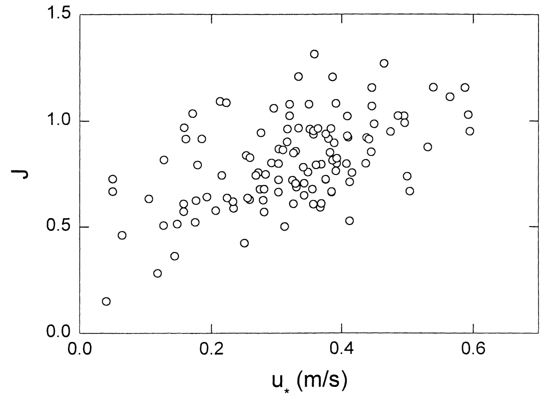

Fig. 5. Daytime energy flux ratio $J = (\rho c_p \overline{w'T'} + \lambda \overline{w'\rho_v'})/(R_n - S - G)$ plotted as a function of the friction velocity u_* at BR for the height of 23.0 m above the ground.

to be stationary, leading to a large mesoscale flux (essentially the mass flow component in Eq. (4)) that the conventional tower instruments are unable to capture. This may indeed be the reason why tower flux research groups often observe an energy deficit (I positive) and rarely an energy surplus (I negative) under highly convective conditions. Clearly data quality of other scalar fluxes must also be suspected if a large energy imbalance occurs.

The influence of the stationary cell-like structure on energy balance is illustrated by BR data in Fig. 5. The ratio of the sum of eddy fluxes of sensible heat and latent heat to the available energy flux is significantly lower than unity at low friction velocity values and approaches unity as the friction velocity increases, presumably because strong mechanical turbulence does not permit the cell-like structure to take shape. A similar relationship has also been found for the PA site (T.A. Black, personal communications) and is suggested by the observation of Barr et al. (1994).

4.1.2. Synoptic scale subsidence

Subsidence at synoptic scales (1000 km) will occur under fair weather conditions since they are associated with synoptic high pressure systems. Subsidence has been shown to play an important role in the evolution of the nocturnal boundary layer, particularly on nights free of clouds and with strong radiative cooling (Carlson and Stull, 1986). Its direct role in the forest-air exchange is rather limited. With δ values of -2000 and 500 J m^{-3} for daytime and nighttime, respectively, a typical subsidence velocity of -0.04 cm s^{-1} at the height of 40 m will give rise to small equivalent energy fluxes of 0.8 and -0.2 W m^{-2}, respectively. On the other hand, fair weather conditions will favor the formation of strong thermal convection and local thermal circulations, thus modifying the energy balance and trace gas exchange indirectly.

4.1.3. Local circulations

Local thermal circulations (scale ranging from several km to several tens of km) driven by surface heterogeneity have been observed over the HAPEX-MOBILHY study site dominated by forest and cropland landscapes (Mahrt and Ek, 1993), areas near a large river (Oliveira and Fitzjarrald, 1994), irrigated farms surrounded by drier land (Doran and Colleagues, 1992; Mahrt et al., 1994), and areas near a boreal lake (Sun et al., 1997). The work at HAPEX-MOBILHY is particularly relevant to the present study. Mahrt and Ek (1993) found that a persistent ascending motion exists in the daytime over the HAPEX-MOBILHY forest where a micrometeorological tower was located, with a mean value $\bar{w} = 2$ cm s^{-1} at a height of 125 m above the ground. The observed pattern is in good agreement with numerical simulations for the same study area (Andre et al., 1989; Pinty et al., 1989). The associated horizontal flow convergence will supply sensible heat and latent heat to the forest around the tower, or in other words, the mass flow component in the energy balance equation Eq. (8) should be negative because the thermodynamic property δ is generally negative in the daytime. It is perhaps not a surprise that the sum of EC sensible and latent heat fluxes observed over the forest should exceed the net radiation flux (Shuttleworth et al., 1988).

It is also instructive to compare the advection and mass flow terms using the HAPEX-MOBILHY data. The horizontal gradients of temperature and humidity are 0.01°C km^{-1} and -0.01 g m^{-3} km^{-1}, respectively [Fig. 4 of Mahrt and Ek (1993)]. This means that the advective fluxes of sensible heat and latent heat are about 0.05 and -0.03 W m^{-2} at an ambient wind speed of 4 m s^{-1}. On the other hand, the mass flow component due to the horizontal convergence will lead to a much larger equivalent energy flux of -40 W m^{-2} using $\bar{w}$=2 cm s^{-1} and δ=-2000 J m^{-3}.

Direct observational evidence of the nocturnal phase of local thermal circulations is scanty (Sun et al., 1997). One of the most important flow types is drainage flow on undulating terrain because micrometeorological sites are rarely flat. Drainage flow has been proposed as a possible mechanism that depletes the CO_2-enriched air below the EC level (Grace et al., 1996). The simple scale argument of Wyngaard and Kosovic (1994) and model simulations by Brost and Wyngaard (1978) show that the slope effect is significant even at a site with a terrain slope as small as 1.5 parts per thousand. By the continuity requirement, the divergence along the slope due to the gravitational acceleration must be compensated by a downward air motion ($\bar{w} < 0$). Mahrt (1982) has derived the following relation for the along-slope wind component ($\bar{\bar{u}}$) on the assumption that the downslope advection is balanced by the gravitational force,

$$\bar{\bar{u}} = \left(\frac{g\bar{\bar{\theta}}}{\theta} L \sin\alpha \right)^{1/2} \tag{9}$$

where g is gravitational acceleration, θ is potential temperature, $\bar{\bar{\theta}}$ is the average potential temperature depression in the flow, L is downslope distance, and α is slope angle. Mahrt (1982) considers this to be a maximum value in that surface drag, entrainment and along-slope pressure gradients all normally reduce the magnitude of $\bar{\bar{u}}$. With typical values of 5 K, 1000 m and 1° for $\bar{\bar{\theta}}$, L and α, the above equation yields a divergence rate of 8×10^{-4} s^{-1}, or a mean vertical velocity of -3 cm s^{-1} at the 40 m height. This crude order-of-magnitude estimate suggests that the mass flow component in Eq. (4) is indeed very important, even if in reality $\bar{w}$ is only 10% of this upper limit.

The area at a 20 km scale around the PA micrometeorological tower is sloped from northwest to southeast at an angle of roughly 1°. Drainage flow is evident at nights of low wind speed. Fig. 6 is a typical example showing the persistent negative mean vertical velocity at both EC levels at night (mean nighttime wind speed 2.7 m s^{-1}). The diurnal pattern becomes obscure when the averaged nighttime wind speed is greater than 3.0 m s^{-1}. The existence of drainage flow is further supported by the nighttime $\bar{w}$ frequency distribution which is significantly skewed towards negative values as opposed to the symmetric distribution during the daytime (Fig. 7). The median

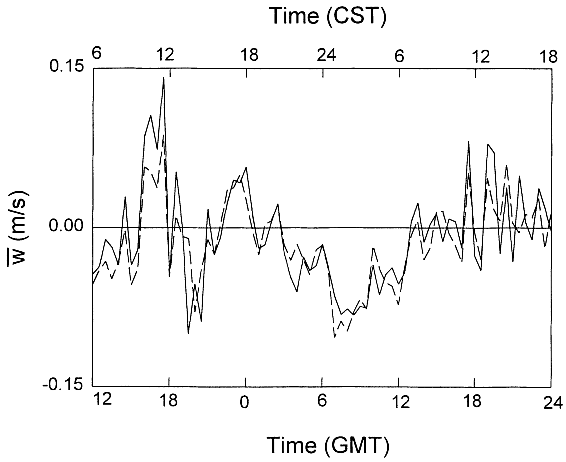

Fig. 6. Diurnal variations of the corrected mean vertical velocities observed at the heights of 39.1 m (solid line) and 27.7 m (dash line) above the ground at PA on August 31–September 1, 1994.

value of the nighttime observations is $-1.0\ \mathrm{cm\ s^{-1}}$, which agrees in order of magnitude with the estimate using Mahrt's model.

4.2. Implications for CO_2 flux observation

To explore the role of the above mechanisms in the forest-air exchange of CO_2, we begin with a plot of the diurnal variations in the CO_2 concentration gradient $\delta\bar{C} = \bar{C}_r - \langle\bar{C}\rangle$ observed at PA (Fig. 8). Data are

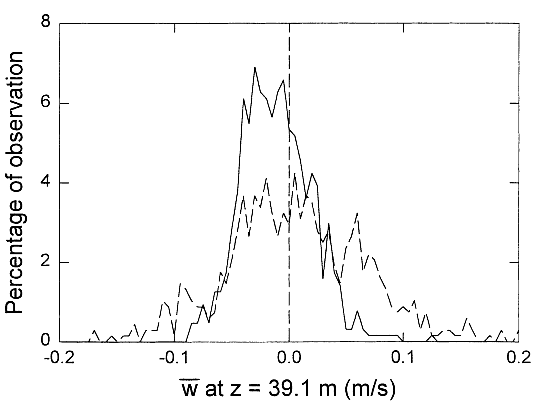

Fig. 7. Frequency distribution of the corrected 30 min mean vertical velocity at the height of 39.1 m above the ground at PA from midnight (22–04 CST, solid line) and midday (10–16 CST, dash line) periods. Percentage of observation is calculated over $0.1\ \mathrm{cm\ s^{-1}}$ intervals.

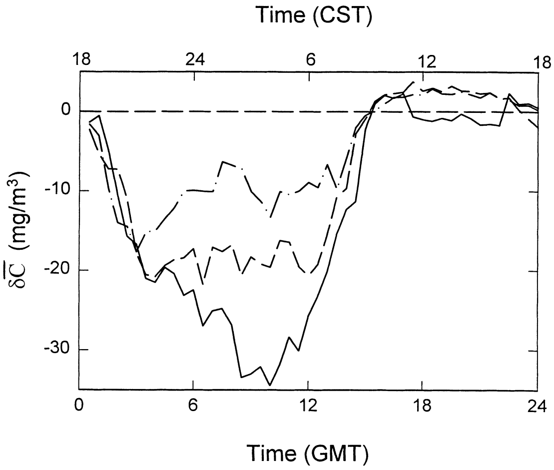

Fig. 8. Ensemble averages of the CO_2 concentration gradient $\delta\bar{C} = \bar{C}_r - \langle\bar{C}\rangle$, where $\bar{C}_r$ is the concentration at the EC height (39.1 m above the ground): solid line, mean nighttime wind speed less than $2.2\ \mathrm{m\ s^{-1}}$; dash line, wind speed between 2.2 and $3.0\ \mathrm{m\ s^{-1}}$; dash–dot line, wind speed greater than $3.0\ \mathrm{m\ s^{-1}}$.

sorted into three wind speed classes: mean nighttime wind speed less than $2.2\ \mathrm{m\ s^{-1}}$, wind speed between 2.2 and $3.0\ \mathrm{m\ s^{-1}}$ and wind speed greater than $3.0\ \mathrm{m\ s^{-1}}$. The last class corresponds roughly to the wind criterion used by Black et al. (1996) in screening nighttime CO_2 flux data for quantifying the annual NEE of this forest. The average midnight EC CO_2 fluxes are 0.11, 0.12 and 0.15 mg $\mathrm{m^{-2}\ s^{-1}}$ for the three classes, respectively. The value under light wind conditions does not reflect the actual NEE of the forest because under such conditions drainage flow will occur. If $\bar{w}_r = -1.0\ \mathrm{cm\ s^{-1}}$ is typical of the drainage flow under light wind conditions, the mass flow component around midnight will amount to 0.3 mg CO_2 $\mathrm{m^{-2}\ s^{-1}}$, which is greater than the EC flux of 0.15 mg CO_2 $\mathrm{m^{-2}\ s^{-1}}$ obtained during nights of strongwinds. This raises the possibility that even under strong ambient wind conditions drainage flow may still play a role in the forest-air exchange of CO_2, although the exact magnitude is difficult to quantify.

One major uncertainty in long-term flux observations lies in the problem of selectively systematic errors (errors that apply to only part of the daily cycle, Moncrieff et al., 1996). Errors arising from neglect of the mass flow component are selectively systematic simply because the concentration gradient is greater at night than during the day (Fig. 8). As an example,

Table 1
Typical values of the mean vertical velocity $\bar{w}_r$ (cm s^{-1}) for three motion types, the corresponding values of the mass flow component of CO_2 $\delta F_c = \bar{w}_r(\bar{C}_r - \langle\bar{C}\rangle)$ (mg(CO_2)m^{-2} s^{-1}) and values extrapolated to the whole growing season (δNEE, t C ha^{-1} y^{-1}). Also given is the typical horizontal scale for each motion type (km)

Motion type	Scale	Night (18–09 CST)		Day (09–18 CST)		
		$\bar{w}_r$	δF_c	$\bar{w}_r$	δF_c	δNEE
Synoptic subsidence	1000	−0.04	6×10^{-3}	−0.04	-5×10^{-4}	0.09
Thermal circulation	10	−1	0.15	1	0.012	2.57
Convection	1	0	0	−5	−0.06	−0.06

Table 1 provides an assessment of the mass flow component for the PA forest resulting from the three flow divergence/convergence mechanisms discussed above. The mean CO_2 gradients are $\delta\bar{C} = 1.2$ and -15.0 mg m^{-3} for daytime and nighttime, respectively, based on the data presented in Fig. 8. Stationary cell-like convection is assumed to occur 10% of the daytime. For the purpose of comparison with the NEE value of -3.5 t C ha^{-1} y^{-1} obtained previously (Black et al., 1996), short-term assessment is extrapolated to the whole growing season (110 days). The usual sign convention is adopted here: a negative (positive) flux value indicates CO_2 removal (release) by the forest. Of the three flow types, thermal circulations are the most important one for the long-term flux observations. The error resulting from neglect of the mass flow is as large as the past assessment of NEE itself, emphasizing the need for a better understanding of the dynamics of the circulations and the need for means to measure the vertical velocity accurately.

There are of course numerous reasons why the assessment in Table 1 should be illustrative rather than precise. Some of the problems are: (a) variations due to short-term disturbances such as downdrafts during precipitation events and updrafts in a frontal system; (b) disturbance to the streamlines by topographic forcing; and (c) uncertainties about the persistence of the thermal circulations. Problem (a) is a source of errors at short timescales (hours to days) but as with thermal convection under fair weather, is probably not a major issue in long-term observations. Problem (b) is wind direction dependent. The wind tunnel study of Finnigan and Brunet (1995) shows that the mean streamlines over tall vegetation on hills can depart significantly from the terrain surface and thus the mass flow effect can be significant, although its magnitude is yet to be quantified. Regarding problem (c), uncertainties with the daytime phase of the circulation are not as important because the vertical CO_2 gradient is very small, as shown at the PA forest (Fig. 8). The validity of assuming a constant vertical velocity for all nights may be questionable because under conditions of strong ambient wind, drainage flow is less likely to be detected. Additionally, mechanical mixing under such conditions will reduce the vertical gradient (Fig. 8) and therefore the mass flow component considerably. Selective use of the nighttime flux data as recommended by Wofsy et al. (1993) and adopted by other groups should provide an assessment of the annual NEE more accurate than that obtained by simply adding fluxes of all periods. (The study of Grace et al., 1995 appears to be an exception because they did not find evidence of drainage flow at their forest.) On the other hand, aircraft observations by Mahrt and Ek (1993) suggest that a persistent thermal circulation pattern can exist over a heterogeneous surface with a patch size of the order of 25 km, even though the area near the center of each patch meets the usual micrometeorological site selection criteria.

5. Conclusions

It is shown from first principles (mass conservation and continuity equations) that NEE should consist of three components, storage below the height of observation, eddy flux and a mass flow component arising from horizontal flow convergence/divergence or a non-zero mean vertical velocity (Eq. (4)). The last term, unaccounted for in previous studies of surface–air exchanges, becomes important over tall vegetation and at times when the vertical gradient of the atmospheric constituent is large, as is the case with CO_2 in forests at night. Experimental evidence is presented to support the postulation that the mass flow component is responsible for the large run-to-run variations in eddy fluxes, the problem with energy balance closure, and the apparent low flux values at night under stable stratifications.

Three mechanisms responsible for the non-zero mean vertical velocity are discussed. Of these, drainage flow on undulating terrain is the most important one for long-term flux observations because only a slight terrain slope is required to trigger the flow. It is suggested from the data obtained at the boreal forest that without proper consideration of the drainage flow, the assessment of annual uptake of CO_2 could be biased significantly toward higher values.

The utility of Eq. (4) is limited at present by the fact that it calls for techniques that can measure precisely (within 0.1 cm s^{-1}) the mean vertical velocity at the height of EC observations. While uncertainties also remain with regard to other problems reviewed in the introduction section and in a recent survey study by Mahrt (1998), it is argued that the mass flow component is a fundamental issue in observational studies of forest-air exchanges because in reality no ideal sites (horizontally uniform and perfectly flat) exist. Additionally, even if a site meets the usual fetch criteria, it may still be subject to thermal circulations driven by land surface heterogeneity at scales much larger than the scale of micrometeorology.

Acknowledgements

A number of ideas presented in this paper were prompted by a discussion with Drs. T.A. Black, R.L. Desjardins, L. Mahrt, J. Sun, and S.B. Verma. The author thanks Drs. G. den Hartog and H.H. Neumann for providing the eddy correlation and profile data for the Prince Albert forest. Constructive comments by Dr. L. Mahrt on an earlier draft of the paper are gratefully acknowledged. This work was supported by the US National Science Foundation through grant ATM-9629497.

References

Andre, J.C., Bougeault, P., Mafouf, J.-F., Mascart, P., Noilhan, J., Pinty, J.-P., 1989. Impact of forests on mesoscale meteorology. Philos. Trans. Roy. Soc. London B324, 407–422.

Avissar, R., Chen, F., 1993. Development and analysis of prognostic equations for mesoscale kinetic energy and mesoscale (subgrid scale) fluxes for large-scale atmospheric models. J. Atmos. Sci. 22, 3751–3774.

Baldocchi, D.D., Harley, P., 1995. Scaling carbon dioxide and water vapor exchange from leaf to canopy in a deciduous forest: model testing and application. Plant, Cell and Environ. 18, 1157–1173.

Barr, A.G., King, K.M., Gillespie, T.J., den Hartog, G., Neumann, H.H., 1994. A comparison of Bowen ratio and eddy correlation sensible and latent heat flux measurements above deciduous forest. Bound.-Layer Meteorol. 71, 21–41.

Black, T.A., den Hartog, G., Neumann, H.H., Blanken, P.D., Yang, P.C., Russell, C., Nesic, Z., Lee, X., Chen, S.G., Staebler, R., Novak, M.D., 1996. Annual cycles of water vapour and carbon dioxide fluxes in and above a boreal aspen forest. Global Change Biology 2, 219–229.

Blanken, P.D., Black, T.A., Yang, P.C., den Hartog, G., Neumann, H.H., Nesic, Z., Staebler, R., Novak, M.D., Lee, X., 1997. Energy balance and canopy conductance of a boreal aspen forest: partitioning overstory and understory components, J. Geophys. Res. 102D, 28915–28927.

Brost, R.A., Wyngaard, J.C., 1978. A model study of the stably stratified planetary boundary layer. J. Atmos. Sci. 35, 1427–1440.

Carlson, M., Stull, R.B., 1986. Subsidence in the nocturnal boundary layer. J. Climat. Appl. Meteorol. 25, 1088–1099.

Doran, J.C. and Colleagues, 1992. The Boardman regional flux experiment, Bull. Am. Meteorol. Soc. 73, 1785–1795.

Emanuel, K., 1994. Atmospheric Convection. Oxford University Press, Oxford.

Finnigan, J.J., Brunet, Y., 1995. Turbulent airflow in forests on flat and hilly terrain. In: Coutts, M.P., Grace, J. (Eds.), Wind and Trees. Cambridge University Press, London.

Finnigan, J.J., 1985. Turbulent transport in flexible plant canopies. In: Hutchison, B.A., Hicks, B.B. (Eds.), The Forest–Atmosphere Interactions, D. Reidel, The Netherlands.

Fitzjarrald, D.R., Moore, K.E., 1994. Growing season boundary layer climate and surface exchanges in a subarctic lichen woodland. J. Geophys. Res. 99, 1899–1917.

Fuentes, J.D., Gillespie, T.J., den Hartog, G., Neumann, H.H., 1992. Ozone deposition onto a deciduous forest during dry and wet conditions. Agric. For. Meteorol. 62, 1–18.

Garratt, J.R., 1992. The Atmospheric Boundary Layer. Cambridge University Press, London.

Garstang, M., Ulanski, S., Greco, S., Scala, J., Swap, R., Fitzjarrald, D., Martin, D., Browell, E., Shipman, M., Connors, V., Harriss, R., Talbot, R., 1990. The Amazon boundary-layer experiment (ABLE 2B): a meteorological perspective. Bull. Am. Meteorol. Soc. 71, 19–32.

Goulden, M.L., Munger, J.W., Fan, S.-M., Daube, B.C., Wofsy, S.C., 1996a. Exchange of carbon dioxide by a deciduous forest: response to interannual climate variability Science 271, 1576–1578.

Goulden, M.L., Munger, J.W., Fan, S.-M., Daube, B.C., Wofsy, S.C., 1996b. Measurements of carbon sequestration by long-term eddy covariance: methods and a critical evaluation of accuracy Global Change Biology 2, 168–182.

Grace, J., Malhi, Y., LIoyd, J., McIntyre, J., Miranda, A.C., Meir, P., Miranda, H.S., 1996. The use of eddy covariance to infer the net carbon dioxide uptake of Brazilian rain forest. Global Change Biology 2, 209–217.

Grace, J., LIoyd, J., McIntyre, J., Miranda, A.C., Meir, P., Miranda, H.S., Nobre, C., Moncrieff, J., Masheder, J., Malhi, Y., Wright, I., Gash, J., 1995. Carbon dioxide uptake by an undisturbed tropical rain forest in southwest Amazonia, 1992–1993. Science 270, 778–780.

Guenther, A., Baugh, W., Davis, K., Hampton, G., Harley, P., Klinger, L., Vierling, L., Zimmerman, P., Allwine, E., Dilts, S., Lamb, B., Westbeg, H., Baldocchi, D., Geron, C., Pierce, T., 1996. Isoprene fluxes measured by enclosure, relaxed eddy accumulation, surface layer gradient, mixed layer gradient and mixed layer mass balance techniques. J. Geophys. Res. 101D, 18555–18567.

Hollinger, D.Y., Kelliher, F.M., Byers, J.N., Hunt, J.E., McSeveny, T.M., Weir, P.L., 1994. Carbon dioxide exchange between an undisturbed old-growth temperate forest and the atmosphere. Ecology 75, 134–150.

Jarvis, P.G., Massheder, J.M., Hale, S.E., Moncrieff, J.B., Rayment, M., Scott, S.C., 1997. Seasonal variation of carbon dioxide, water vapor and energy exchanges of a boreal spruce forest, J. Geophys. Res. 102D, 28953–28966.

Lee, X., Neumann, H.H., den Hartog, G., Fuentes, J.D., Black, T.A., Mickle, R.E., Yang, P.C., Blanken, P.D., 1997. Observation of gravity waves in a boreal forest. Bound.-Layer Meteorol. 84, 383–398.

Lee, X., Black, T.A., 1993a. Atmospheric turbulence within and above a Douglas-fir stand. Part I. Statistical properties of the velocity field Bound.-Layer Meteorol. 64, 149–174.

Lee, X., Black, T.A., 1993b. Atmospheric turbulence within and above a Douglas-fir stand. Part II. Eddy fluxes of sensible heat and water vapor Bound.-Layer Meteorol. 64, 369–389.

Lindberg, S.E., Hanson, P.J., Meyers, T.P., Kim, K.-H., 1997. Air/surface exchange of mercury vapor over forests, the need for a reassessment of continental biogenic emissions, Atmospheric Environment, in press.

Leuning, R., Judd, M.J., 1996. The relative merits of open- and closed-path analysers for measurement of eddy fluxes. Global Change Biology 2, 241–253.

Mahrt, L., 1998. Flux sampling errors for aircraft and towers. J. Atmos. Sci. Oceanic Tech. 15, 416–429.

Mahrt, L., Sun, J., 1995. Dependence of surface exchange coefficients on averaging scale and grid size. Quart. J. R. Meteorol. Soc. 121, 1835–1852.

Mahrt, L., Sun, J., Vickers, D., MacPherson, J.I., Pederson, J.R., Desjardins, R.L., 1994. Observations of fluxes and inland breezes over a heterogeneous surface. J. Atmos. Sci. 51, 2484–2499.

Mahrt, L., Ek, M., Spatial variability of turbulence fluxes and roughness lengths in HAPEX-MOBILHY, Bound.-Layer Meteorol. 65, 381–400.

Mahrt, L., 1982. Momentum balance of gravity flows. J. Atm. Sci. 39, 2701–2711.

Moeng, C.-H., 1984. A large eddy simulation model for the study of planetary boundary-layer turbulence. J. Atmos. Sci. 41, 2052–2062.

Moncrieff, J.B., Malhi, Y., Leuning, R., 1996. The propagation of errors in long-term measurements of land–atmosphere fluxes of carbon dioxide and water. Global Change Biology 2, 231–240.

Monteith, J.L., Unsworth, M.H., 1990. Principles of Environmental Physics. Edward Arnold, New York.

Moore, C.J., Hicks, B.B., 1973. The heat budget of a pine forest. In: First Australasian Conference on Heat and Mass Transfer, pp. 57–64, Monash University, Melbourne, Australia.

Moore, K.E., Fitzjarrald, D.R., Sakai, R.K., Goulden, M.L., Munger, J.W., Wofsy, S.C., 1996. Seasonal variation in radiative and turbulent exchange at a deciduous forest in Central Massachusetts. J. Appl. Meteorol. 35, 122–134.

Oliveira, A.P., Fitzjarrald, D.R., 1994. The Amazon river breeze and the local boundary layer. Part I. Observations. Bound.-Layer Meteorol. 63, 141–162.

Pinty, J.-P., Mascart, P., Richard, E., Rosset, R., 1989. An investigation of mesoscale flows induced by vegetation inhomogeneities using an evapotranspiration model calibrated against HAPEX-MOBILHY data. J. Appl. Meteorol. 28, 976–992.

Schmidt, H., Schumann, U., 1989. Coherent structure of the convective boundary layer derived from large eddy simulations. J. Fluid Mech. 200, 511–562.

Segal, M., Avissar, R., McCumber, M.C., Pielke, R.A., 1988. Evaluation of vegetation effects on the generation and modification of mesoscale circulations. J. Atmos. Sci. 45, 2268–2292.

Shen, S., Leclerc, M.Y., 1995. How large must surface inhomogeneities be before they influence the convective boundary layer structure: a case study. Quart. J. R. Meteorol. Soc. 121, 1201–1228.

Shuttleworth, W.J., Gash, J.H.C., LLoyd, C.R., McNeill, D.D., Moore, C.J., Wallace, J.S., 1988. An integrated micrometeorological system for evaporation measurement. Agric. For. Meteorol. 43, 295–317.

Stull, R.B., 1988. An Introduction to Boundary Layer Meteorology. Kluwer Academic Publishers, Dordrecht.

Sun, J., Desjardins, R., Mahrt, L., MacPherson, I., 1997. Transport of carbon dioxide, water vapor and ozone over Candle Lake, J. Geophys. Res., in press.

Thompson, N., 1979. Turbulence measurements above a pine forest. Bound.-Layer Meteorol. 16, 293–310.

Verma, S.B., Baldocchi, D.D., Anderson, D.E., Matt, D.R., Clement, R.J., 1986. Eddy fluxes of CO_2, water vapor, and sensible heat over a deciduous forest. Bound.-Layer Meteorol. 36, 71–91.

Wallace, J.M., Hobbs, P.V., 1977. Atmospheric Science: An Introductory Survey. Academic Press, New York.

Wofsy, S.C., Goulden, M.L., Munger, J.W., Fan, S.-M., Bakwin, P.S., Daube, B.C., Bassow, S.L., Bazzaz, F.A., 1993. Net exchange of CO_2 in a mid-latitude forest. Science 260, 1314–1317.

Wyngaard, J., Kosovic, B., 1994. Similarity of structure function parameters in the stably stratified boundary layer. Bound.-Layer Meteorol. 71, 277–296.